19th Australasian Fluid Mechanics Conference
Melbourne, Australia
8-11 December 2014

Simulation and Experimental Testing of Leonardo da Vinci's Helical Rotor

G. E. Dorrington[1], H. Ogawa[1], J. McCarthy[1], and R. Carrese[2]

[1]School of Aerospace, Mechanical and Manufacturing Engineering,
RMIT University, Victoria 3083, Australia.
[2]LEAP Australia,
750 Blackburn Rd, Clayton North, VIC 3168, Australia.

Abstract

Preliminary thrust tests carried-out on a 0.5 metre diameter, helical rotor based on a sketch by Leonardo da Vinci are presented, along with the results of computational flow simulation. Some of the key geometric variables that define the helical rotor and their influence on the maximum achievable thrust level are also discussed. It is concluded that with sufficient input power, da Vinci's helical rotorcraft could achieve hovering flight; however, the technical challenges involved in a developing a free-flight hovering demonstrator would be formidable.

Introduction

About 500 years ago, Leonardo da Vinci, produced a famous sketch of a machine presumably intended to be capable of free-flight with vertical take-off and landing, figure 1. Surprisingly, to date, there have been few studies with any in-depth supporting engineering analyses concerned with the feasibility of such inspired, historically-significant inventions [4].

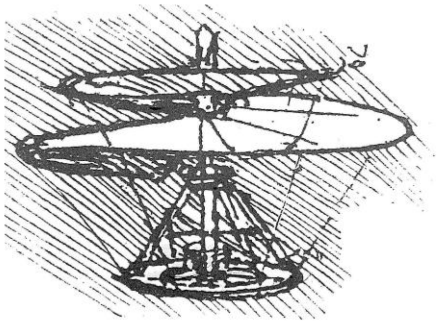

Figure 1. Helical-rotorcraft sketched by Leonardo da Vinci *circa* 1500.

In order to investigate the performance of a similar helical rotorcraft, a 0.5 m diameter helical rotor was 3D printed in polycarbonate. The geometry of the rotor was only intended to be a first approximation of figure 1. The rotor was spun by a direct-drive electric motor up to approximately 3000 rpm, and its vertical thrust was measured using a load cell mounted on a fixed pedestal. The results of this thrust test were then compared with simulated flow predictions using ANSYS CFX software.

Project Motivation and Some Historical Remarks

There are no recorded statements by da Vinci regarding the sketch shown in figure 1. Some enthusiasts have assumed that da Vinci envisaged that this helical rotorcraft would have been necessarily human-powered. However, it could be speculated that da Vinci would have known about Heron's *Aerolipile* and consequently considered a variant of that turbine as a possible power source. The interesting debate that then emerges is: whether, or not, this helical rotorcraft would have been capable of hovering (regardless of consideration of power source and material technology constraints *circa* 1500). This debate then gives rise to the following educational challenge: with current technology, is it possible to demonstrate the free-hover of a similar helical rotorcraft? In order to try to address this question and challenge, it was decided that any numerical flow simulation would need to be supported by experimental test results.

Da Vinci's helical rotorcraft may have been inspired by Archimedes' screw, which is well-known to be capable of inducing flows when shrouded within a duct, but which may be relatively ineffective when unshrouded. Early drawings of Bushnell's one-person submarine, *Turtle* (1776), depict unshrouded, double-turn Archimedes screws, but it is unclear whether the *Turtle* was actually tested using such helical screws. Around 1800-1850 other unshrouded Archimedes-type screws were also tested as potential dirigible propulsion schemes. An unshrouded, single-turn helical propeller (with a pitch of about 3m and a diameter of 1.75 m) was used successfully for the propulsion of the ship *Archimedes* in 1839 [1].

Geometry and Manufacture of Printed Helical Rotor

There are several difficulties involved in translating the sketch in figure 1, into a well-defined geometry, e.g., da Vinci only provides one view with a perspective projection.

The geometry of the final printed helical rotor is depicted in figure 2. A one-and-a-half-turn helix was selected as being representative where the outer radius was defined by,

$$r = r_{min} + (r_{max} - r_{min})\theta/(3\pi) \quad (1)$$

where r_{min} = 175 mm and r_{max} = 250 mm. Although da Vinci's sketch (figure 1) apparently depicts the helical lifting surface to have both dihedral (upper turn) and anhedral (lower turn), for simplicity the swept rotor blade plane was assumed to be orthogonal to the rotor axis, i.e., Γ was fixed at zero. The pitch of the rotor was set at $z \cong 100$ mm. The resulting helix taper angle was $\beta \cong 23$ degrees, figure 2.

The rotor was printed using a Stratasys FORTUS 900 within RMIT's Advanced Manufacturing Precinct (AMP). The rotor was orientated with print layer orthogonal to the axis, using T12 tips which produce 0.17 mm slices. The lifting surface thickness of the polycarbonate material was approximately 5 mm near the central axis tapering down to about 2 mm at the outer radius. Some reinforcement stakes were added to the lower rear surface to prevent some trailing flutter that was observed in an earlier, thinner and lighter rotor. The rotor was axially mass-balanced by designing-in added thickness in certain regions of helix surface.

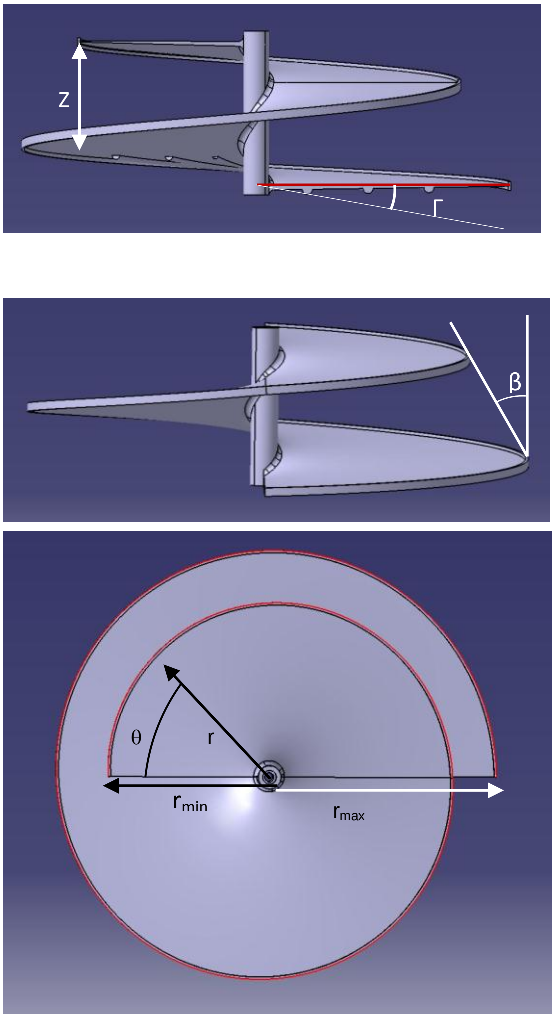

Figure 2. Geometry of printed helical rotor, see acknowledgements.

Basic Performance Analysis

The shaft power input, P_0, required for a conventional multi-bladed rotor to achieve a given static hover thrust, T_0, may be predicted using the standard coefficient equation [2],

$$C_P = \kappa C_T^{3/2} / \sqrt{2} + \sigma c_{d0} / 8 \qquad (2)$$

where: $C_P = P_0 / \rho \pi r_{max}^2 (\Omega r_{max})^3$ is the power coefficient of the rotor in an atmosphere with density ρ turning at angular velocity, Ω; $C_T = T_0 / \rho \pi r_{max}^2 (\Omega r_{max})^2$ is the thrust coefficient; $\sigma = Nc / \pi r_{max}$ is the blade solidity and c_{d0} is the profile blade drag coefficient based on the rotor chord, c. Typically, the magnitude of profile term on the right-hand side of equation (2) is about 30% that of the induced term and $\sigma \leq 0.1$.

In the case of the printed helical rotor, $N = 1$ and the effective chord is $c = 3\pi(r_{min} + r_{max})/2$, i.e., $\sigma \cong 3$. In other words, the profile term of the helical rotor may reasonably be expected to be an order of magnitude larger than the induced term. This strongly suggests that for the same angular speed and static hover thrust requirement, any helical rotor would require a much larger power input than a conventional helicopter rotor, regardless of how well it is designed in terms maintaining a 'healthy' flow.

Experimental Study

Thrust Rig Description

A photograph of the assembled experimental test rig is shown in figure 3. This shows the printed helical rotor attached to a direct drive (ungeared) Hacker Q80 motor that was radio-controlled. The motor is mounted on a JR3 load cell capable of a maximum load capability of 200 N. The load cell is itself mounted on a 1.5 m high steel pedestal that was bolted to a concrete floor in an attempt to reduce vibration levels. The angular speed was measured using a stroboscope. Induced velocity was measured using a pitot tube mounted about 0.5 m below the rotor.

The load cell was calibrated with a 1 N weight. Also, a conventional propeller with similar radius (whose static thrust had been previously measured elsewhere) was tested, in order to ensure there were no electromagnetic interference effects.

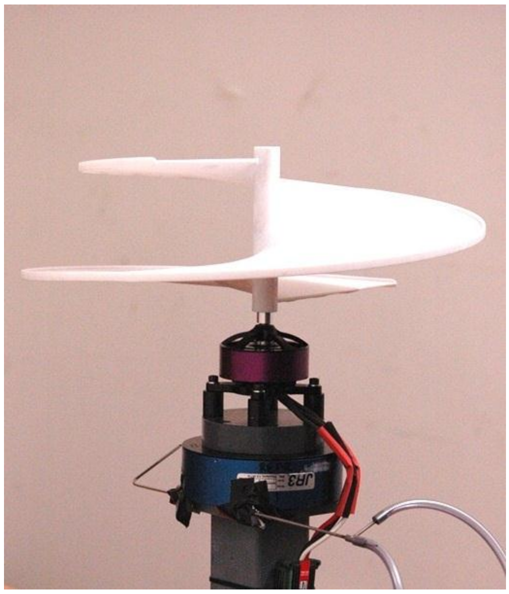

Figure 3. Printed helical rotor test rig, see acknowledgements.

Thrust Rig Measurements

Some sample results of the printed helical rotor tests are shown in Table 1. The Reynolds number is defined here as, $Re = 2\rho\Omega^2 r_{max} / \mu$. The results are well-matched by equation 2, when $c_{d0} \cong 0.006$ and $\sigma = 3$, but, unfortunately, they are not deemed sufficiently accurate to determine the value of the induced drag coefficient, κ.

At the rotor speeds tested, the profile power term dominates, somewhat like a conventional near-windmilling propeller, suggesting that the pitch of the rotor was too low. The induced velocity detected by the pitot was also far lower than would be expected had the flow over helical surface been fully attached.

$Re/10^6$	1.59	2.15	2.29	2.61
$1000C_T$	0.19	0.35	0.39	0.45
$1000C_P$	2.35	2.67	2.72	2.87

Table 1. Sample thrust and power coefficients derived from thrust measurements on the printed helical rotor shown in Figure 2.

It should be noted that these preliminary thrust tests were limited to 3000 rpm, because of concerns of possible break-up of the polycarbonate rotor and excessive vibration-wobble in the steel mounting pedestal. Higher speed tests clearly need to be performed to obtain higher thrust coefficients.

Numerical Simulation

Methodology

The flow simulation was performed using ANSYS CFX (release 15) with the rotational sliding mesh model and the Shear Stress Transport (SST) model including correctional terms for turbulence anisotropy. The mesh was generated with a patch conforming hybrid tetrahedral topology using ANSYS Meshing R15 and non-conformal interfaces at the sliding mesh interface. The SST model is a low-*Re* eddy viscosity turbulence model, which blends *k*-ω in the near wall region and k-ε in the freestream, providing good behaviour in adverse pressure gradients and separating flow.

Results

Some images of the computational simulation of flow-field are shown in Figure 4 and Figure 5. As expected the flow is far from being axially-symmetric, and the resulting centre of pressure position has an unsteady fluctuation. High circumferential flow velocities exist below the helical surface suggesting unnecessary loss of lift. Figure 5 depicts the contours of the vertical flow component along with local flow vectors.

The simulated (time-averaged) thrust was found to exceed the experimental measurements discussed above, but the trend of increasing C_T with *Re* (Table 1) was matched for $Re > 10^6$.

Discussion

We recognise that simulating da Vinci's rotor has no direct industrial application, but this project involved a number of capability challenges that may be of industry interest. In particular, the complex flow phenomena involved are somewhat similar to those produced by marine propellers, e.g., [3].

One of the main technical challenges involved in developing a free-flight hovering demonstrator will be the construction of sufficiently lightweight helical rotor that is axially mass-balanced. We have started investigating the feasibility of producing a rotor from carbon-fibre composite. Assembling a multi-blade segmented helix appears to be a promising approach, noting that da Vinci drew segmenting lines on the lifting surface.

Conclusions

In this preliminary study the measured and computationally predicted thrust values agreed quite closely, but the angular rotor speeds tested were too low to generate significantly high thrust in order to confidently and accurately predict the performance of a free-flight demonstrator capable of hover.

In order, to achieve higher speed tests at more than one order of magnitude higher input levels, a robust, lightweight composite rotor would be needed. Of course, *circa* 1500, da Vinci would not have been able to realise such demanding power inputs and material strength requirements, but at least this study indicates that a contemporary-technology version of da Vinci's helical rotorcraft capable of free-flight hovering is feasible.

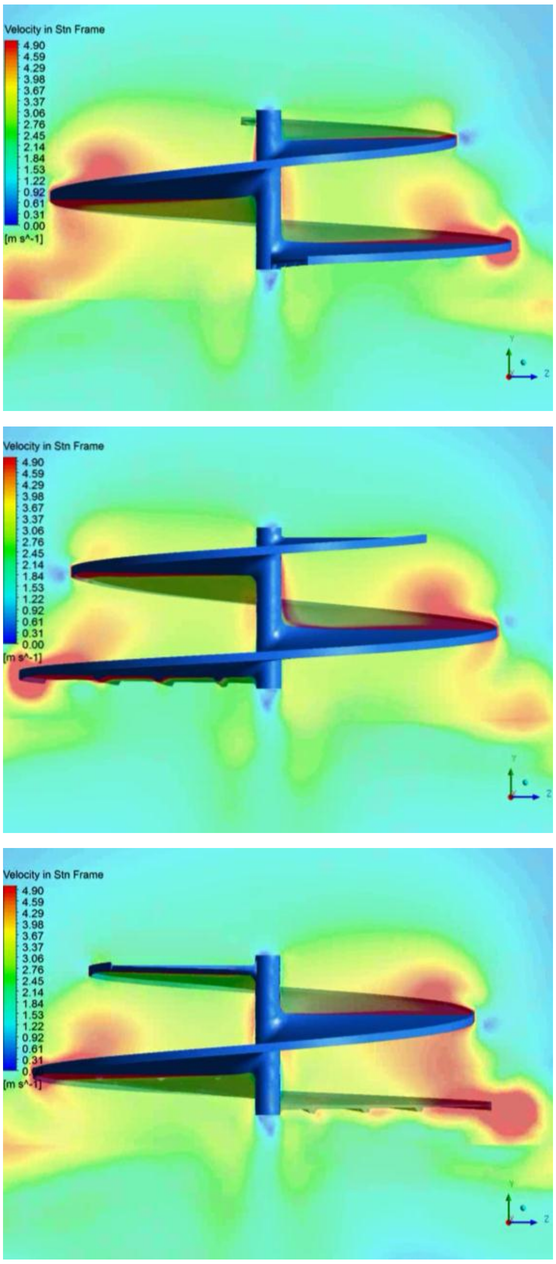

Figure 4. Three snapshots of the simulated unsteady absolute velocity, at a rotor angular speed of 2000 rpm, $Re \cong 1.75 \times 10^6$.

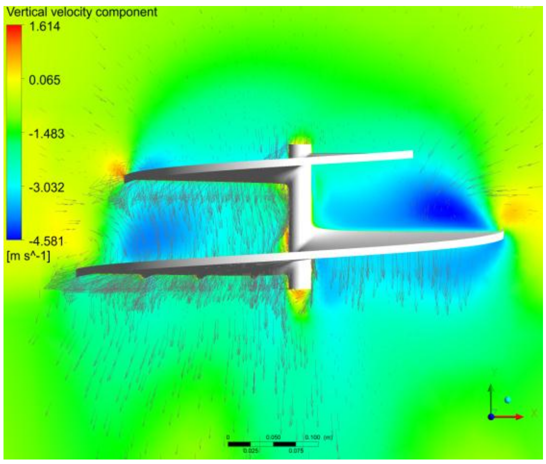

Figure 5. Vertical velocity contours and flow vectors (arrows), at a rotor angular speed of 2000 rpm, $Re \cong 1.75 \times 10^6$.

Acknowledgments

The authors wish to thank: Achim Washington (4th year aerospace student) who generated the rotor CAD geometry; Adrian MacHoy (4th year aerospace student) who performed the thrust tests; Figure 2 is also based on the work of Tim Rudd-Schmidt (3rd year aerospace student); technical support staff including Paul Porter and Albert Maberley for 3D printing in RMIT's AMP and finally but not least, Gil Atkins for assembling the rotor test rig and assisting with the tests.

References

[1] Carlton, J. *Marine Propellers and Propulsion*, Butterworth-Heineman, Oxford, 2nd ed., 2007.

[2] Johnson, W., *Helicopter Theory*, Dover, New York, 1946.

[3] Muscari R., Di Mascio, A. Numerical simulation of the flow past a rotating propeller behind a hull, *2nd Int. Symp. Marine Propulsors SMP'11*, Hamburg, Germany, June 2011.

[4] Zanon, E., *The Book of the Codex on Flight, Leonardo da Vinci*, Leonardo3, Milan, ISBN 978-88-6048-011-8, 2009.